ACI STRUCTURAL JOURNAL TECHNICAL PAPER

Title no. 103-S35

Behavior of Reinforced Concrete T-Beams Strengthened in Shear with Carbon Fiber-Reinforced Polymer—An Experimental Study

by Abdelhak Bousselham and Omar Chaallal

This paper presents results of a wide and extensive experimental investigation on reinforced concrete (RC) T-beams retrofitted in shear with externally bonded carbon fiber-reinforced polymer (CFRP). In total, 22 tests were performed on 4520 mm-long T-beams. The parameters investigated were as follows: 1) the CFRP ratio (that is, the number of CFRP layers); 2) the internal shear steel reinforcement ratio (that is, spacing); and 3) the shear length to the beam's depth ratio, a/d *(that is, deep beam effect). The main objective of the study was to analyze the behavior of RC T-beams strengthened in shear with externally applied CFRP by varying the aforementioned parameters. The results showed that the contribution of the CFRP to the shear resistance is not in proportion to the CFRP thickness (that is, the stiffness) provided, and depends on whether the strengthened beam is reinforced in shear with internal transverse steel reinforcement. Results also confirmed the influence of the ratio* a/d *on the behavior of RC beams retrofitted in shear with external fiber-reinforced polymer (FRP). Finally, comparison of the shear resistance values predicted by ACI 440.2R-02, CSA S806-02, and* fib *TG9.3 guidelines, with the test results clearly indicated that the guidelines fail to capture important aspects, such as the presence of the transverse steel and the ratio* a/d *on the one hand, and overestimates the shear resistance for high FRP thickness (and hence high FRP stiffness), on the other.*

Keywords: polymer; reinforced concrete; shear; strain; strengthening.

INTRODUCTION

One of the techniques used to strengthen existing reinforced concrete (RC) members involves externally bonding fiber reinforced polymer (FRP) composite materials by means of epoxy adhesives. This technique improves the structural performance of a member (Neale 2000; Meier 1995). The wide use of this strengthening method for various structures, including buildings and bridges, has demonstrated its efficiency and its convenience (Bakis et al. 2002; Clarke 2000).

Strengthening of beams and slabs in flexure and confinement of circular columns have been well documented. A review of research studies on shear strengthening, however, revealed that experimental investigations are still needed (Bousselham and Chaallal 2004; Matthys and Triantafillou 2001). Research studies carried out in recent years have provided valuable findings, particularly with regard to the effect of the stiffness of the composite on the shear strength enhancement (Triantafillou and Antonopoulos 2000; Khalifa and Nanni 2000). Other parameters that also influence the shear resistance mechanism, however, were not sufficiently studied (Bousselham and Chaallal 2004). Shear steel reinforcement and shear span to depth ratio (a/d) are examples of such parameters.

To address these areas, the authors conducted a large experimental investigation on the shear performance of RC beams strengthened with externally bonded carbon fiber-reinforced polymer (CFRP) fabric. The parameters of the study were set as follows: 1) the CFRP ratio (that is, the number of CFRP layers); 2) the internal shear steel reinforcement ratio (that is, spacing); and 3) the shear length to the beam depth ratio, a/d (that is, deep beam effect).

The objectives of this paper are as follows:

- To investigate the shear performance, including the mode of failure, of RC beams strengthened with CFRP in terms of the CFRP; the internal transverse steel reinforcement, hereafter called the transverse steel; and the shear span to depth ratios;
- To analyze the behaviour of the CFRP, the internal transverse and longitudinal steel reinforcement, and the concrete struts, while the above parameters are varied; and
- To verify the reliability of ACI 440.2R-02 (ACI Committee 440 2002), CSA S806-02 (Canadian Standards Association 2002), and *fib* TG9.3 (2001), hereafter called the guidelines.

RESEARCH SIGNIFICANCE

Most research studies on shear strengthening with FRP composites are mainly focused on the properties and the performance of the FRP and often involve rectangular beam test specimens of reduced sizes. Also, the lack of data on the strains experienced by the different components (FRP, concrete, and steel) makes it difficult, if not impossible, to fully grasp the prevailing shear resistance mechanisms. The proposed research was targeted to address these and other important aspects. It is believed that the findings of this study contribute to the understanding of the resistance mechanisms involved for RC beams strengthened in shear with externally bonded FRP. This understanding is of paramount importance because it leads to a more rigorous approach toward safer and rational design guidelines.

EXPERIMENTAL PROGRAM

The experimental program (Table 1) involves 22 tests performed on 11 full-scale T-beams. The control specimens, not strengthened with CFRP, are labelled 0L, whereas the specimens retrofitted with CFRP are labelled 0.5L, 1L, or 2L, corresponding to 0.5, 1, and 2 bonded layers of CFRP, respectively. The letters DB (deep beam) and SB (slender

ACI Structural Journal, V. 103, No. 3, May-June 2006.
MS No. 04-129 received April 12, 2005, and reviewed under Institute publication policies. Pertinent discussion including author's closure, if any, will be published in the March-April 2007 *ACI Structural Journal* if the discussion is received by November 1, 2006.

Abdelhak Bousselham *is a PhD candidate in the Department of Construction Engineering, University of Quebec, Ecole de technologie supérieure, Montreal, Quebec, Canada. His research interests include the use of fiber-reinforced polymer composites for strengthening and retrofitting concrete structures.*

ACI member **Omar Chaallal** *is Professor of Construction Engineering, University of Quebec. He is a member of ACI Committee 440, Fiber Reinforced Polymer Reinforcement. His research interests include experimental and analytical research on the use of fiber-reinforced polymer composites for strengthening and retrofitting concrete structures.*

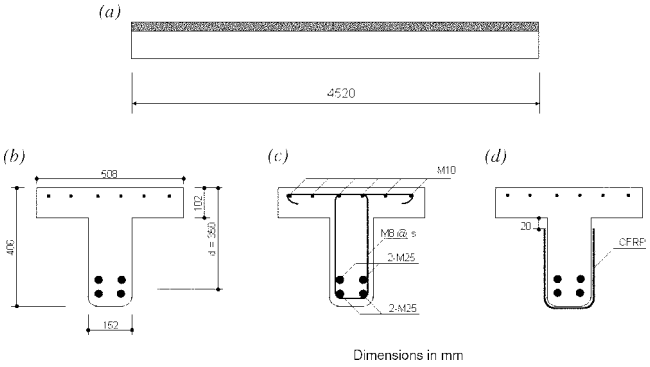

Fig. 1—Details of specimens: (a) elevation; (b) cross section with no transverse steel; (c) cross section with transverse steel; and (d) wrapped cross section.

beam) are used to designate specimens with small and high a/d, respectively. Series S0 is made of specimens with no internal transverse steel reinforcement (that is, no stirrups). Series S1 and S2 correspond to specimens with internal transverse steel stirrups, hereafter called transverse steel, spaced at $s = d/2$ for S1 and $s = d/4$ for S2, where $d = 350$ mm and represents the effective depth of the cross section of the beam. Thus, for instance, Specimen DB-S0-1L features a small a/d, has no transverse steel, and is retrofitted with one layer of CFRP.

Description of specimens

The T-beams are 4520 mm long. The T-section has overall dimensions of 508 mm (width of flange) by 406 mm (total depth). The thickness of the web and the flange are 152 and 102 mm, respectively (Fig. 1). It should be noted that the web was chamfered at the outer corners, thereby easing the high stress concentration in the CFRP at those locations.

The longitudinal steel reinforcement consists of four 25M bars (diameter of 25.2 mm, area of 500 mm^2) laid in two layers at the bottom and six 10M bars (diameter of 10.3 mm, area of 100 mm^2) laid in one layer at the top. The bottom bars are anchored at the support with 90 degree hooks to prevent premature anchorage failure. The internal steel stirrups are 8 mm in diameter (area of 50 mm^2).

The composite material is a bidirectional carbon fiber fabric. It is applied continuously over the test zone in a U-shape around the web. The U-shape has shown to outperform the so-called wing-shape (that is, CFRP on lateral sides only) with regard to debonding (Bousselham and Chaallal 2004). The continuous composite material was selected as it is well suited for intercepting diagonal cracks, which may occur and propagate over a large area within the test zone. The thickness of the CFRP used is 0.060, 0.107, and 0.214 mm for half (0.5L), one (1L), and two layers (2L), respectively. It should be noted that the 0.5L fabric is not manufactured; it was created by manually removing three out of six carbon fiber yarns (for 1 in. wide) from the 1L manufactured fabric.

Table 1—Experimental program

		Deep specimens (DB)			Slender specimens (SB)		
		a/d = 1.5			a/d = 3.0		
		Stirrup spacing			Stirrup spacing		
		S0	$d/2$ (S1)	$d/4$ (S2)	S0	$d/2$ (S1)	$d/4$ (S2)
No. of CFRP layers (L)	0L	BD-S0-0L	DB-S1-0L	DB-S2-0L	SB-S0-0L	SB-S1-0L	SB-S2-0L
	0.5L	DB-S0-0.5L	DB-S1-0.5L	—	SB-S0-0.5L	SB-S1-0.5L	—
	1L	DB-S0-1L	DB-S1-1L	DB-S2-1L	SB-S0-1L	SB-S1-1L	SB-S2-1L
	2L	DB-S0-2L	DB-S1-2L	DB-S2-2L	SB-S0-2L	SB-S1-2L	SB-S2-2L

Table 2—Mixture proportions and properties of concrete

Cement, normal, Type 10, kg/m^3	255
Sand, kg/m^3	1029
Aggregate (maximum 14 mm), kg/m^3	908
Water, kg/m^3	184
Volume of entrained air, %	3
Density, kg/m^3	2360
Slump, mm	40

Table 3—Mechanical properties of steel reinforcement used

	Modulus of elasticity, GPa	Yield stress, MPa	Yield strain, microstrain
25M	200	470	2400
ϕ8	215	650	3000

Table 4—Mechanical properties of CFRP used

Property	Manufacturer (one layer)	Test* (one layer)
Modulus of elasticity, GPa	231	243
Ultimate elongation, %	1.4	1.3
Ultimate stress, MPa	3650	3100

*By testing in laboratory.

Materials

A commercially available concrete was used in this project; it was delivered to the laboratory by a local supplier. The concrete mixture design is presented in Table 2. Standard compression tests on control cylinders revealed a 28-day concrete compressive strength of 25 MPa on average. The steel reinforcing bars used were also tested in tension according to ASTM A 370 standards and results are presented in Table 3. The CFRP composite used is a bidirectional 0 degrees/90 degrees carbon fabric. Table 4 provides the mechanical and elastic properties of the CFRP material as provided by the manufacturer. The CFRP fabric was bonded to the beam surface with an adhesive made of a resin and a hardener, both of which are specially engineered for structural applications and supplied by the CFRP manufacturer.

Test setup

The beam specimens were tested in three-point load flexure. This type of loading was chosen as it allowed two tests to be performed on each specimen: a) one beam end zone is first tested keeping the other overhung and unstressed. In this case the load is applied at a distance $a = 1.5d$ from the nearest support, which corresponds to DB

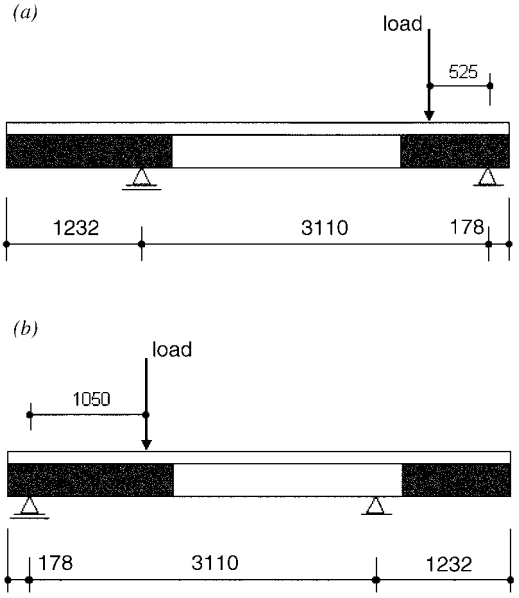

Fig. 2—Setup: (a) test on deep beam; and (b) test on slender beam.

specimen in the nomenclature (Fig. 2); and b) the other beam end zone is tested, but this time it is the end zone already tested that is overhung and unstressed. In this case, the load is applied at a distance $a = 3d$, from the nearest support, which corresponds to a SB specimen in the nomenclature (Fig. 2). The sequence of loading—Specimen DB then SB—was enforced because the specimens and the setup were designed for that order.

Instrumentation

To meet the objective and the scope of the study, a very comprehensive and carefully engineered measuring scheme was adopted for the project.

The vertical displacement was measured at the position under the applied load and at the midspan using linear displacement sensors. The latter were also installed at each side of the supports perpendicular to the flange plan to control any undesired sway or tilt effects. Strain gauges were glued on transverse steel to measure stirrup deformations during the different loading stages and to monitor any yielding (Fig. 3). The deformations experienced by the CFRP wrap were measured using displacement sensors known as crack gauges. These gauges were fixed vertically on the lateral faces of the specimens at the same positions along the longitudinal axis as the strain gauges on the stirrups. Thus, the CFRP and the transverse steel responses can be conveniently compared at the same positions during the different stages of loading.

Likewise, strain gauges were also installed in parallel on the longitudinal steel bars, on and in the concrete and on the CFRP wrap at the tension zone of the specimens (Fig. 3). The data monitored by these gauges will be a valuable tool and will help explain the observed phenomena during the course of the testing and hopefully give a better understanding of the resistance mechanisms.

Testing and recording

The load was applied using a 500 kN capacity MTS hydraulic jack. All the tests were performed under displacement

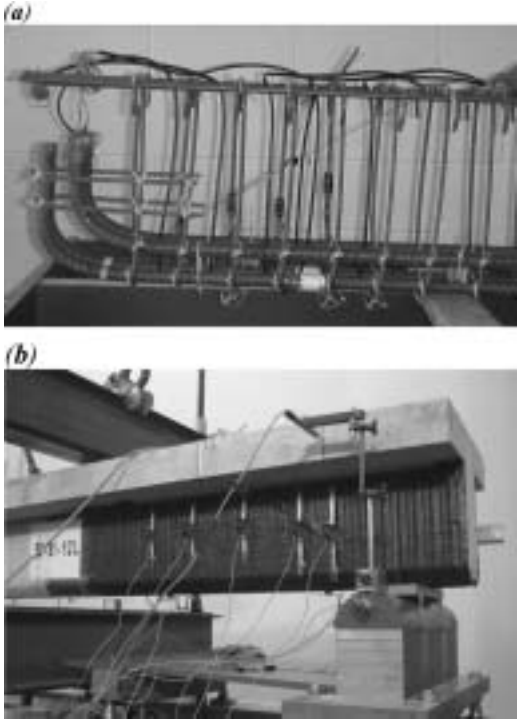

Fig. 3—Instrumentation: (a) strain gauges on transverse and longitudinal steel and embedded in concrete; and (b) crack gauges on CFRP.

control conditions at 2 mm/minute The signals from the gauges and the displacement sensors were captured and monitored using an automatic data acquisition system.

ANALYSIS OF RESULTS

The results related to the global behavior will be presented in terms of: a) the load at rupture and the gain in capacity due to the CFRP; b) the load versus deflection relationship and the gain in stiffness due to the CFRP; and c) the cracking pattern and the failure modes observed. The strain data gathered will be used to study the transverse steel and the CFRP responses as the parameters (that is, the CFRP ratio, the shear steel ratio, and a/d) are varied.

Overall response

Table 5 presents the loads attained at failure; the experimental shear resistance due to concrete, due to the transverse steel, and due to the CFRP; as well as the shear capacity gain due to the CFRP. Note that the values provided in Table 5 were derived on the basis of the following assumptions implicitly admitted in the guidelines: a) the shear resistance due to concrete is the same whether the beam is retrofitted in shear with FRP or not and whether the retrofitted beam is reinforced with transverse steel or not; and b) the contribution of the transverse steel is the same for both retrofitted and nonretrofitted beams.

The results show that the contribution of the CFRP to the shear resistance is greater for the DB specimens with no transverse steel (62% gain) than for the corresponding SB specimens (50% gain). With the transverse steel, these gains drastically decrease to reach 15% on average for the DB specimens, whereas no gain is observed for the SB specimens. This clearly confirms the observations made in recent studies

Table 5—Experimental results

Beam type	Shear steel ratio	No. of CFRP layers	Specimen	Load at rupture, kN	Total resistance, kN	Resistance due to concrete, kN	Resistance due to steel, kN	Resistance due to CFRP, kN	Gain due to CFRP, %	Rupture mode
Deep	S0	0L	DB-S0-0L	214.4	178.2	178.2	0.0	0.0	0.0	Shear
		0.5L	DB-S0-0.5L	322.8	268.2	178.2	0.0	90.1	50.6	Shear
		1L	DB-S0-1L	343.6	285.5	178.2	0.0	107.4	60.3	Shear
		2L	DB-S0-2L	347.8	289.0	178.2	0.0	110.9	62.2	Shear
	S1	0L	DB-S1-0L	389.3	323.5	178.2	145.3	0.0	0.0	Shear
		0.5L	DB-S1-0.5L	373.6	310.5	178.2	145.3	—	—	Test stopped
		1L	DB-S1-1L	427.8	355.5	178.2	145.3	32.0	9.9	Shear
		2L	DB-S1-2L	430.5	357.7	178.2	145.3	34.2	10.6	Shear
	S2	0L	DB-S2-0L	399.2	331.7	178.2	153.6	0.0	0.0	Shear
		1L	DB-S2-1L	468.9	389.7	178.2	153.6	57.9	17.5	Shear
		2L	DB-S2-2L	487.1	404.8	178.2	153.6	73.0	22.0	Shear
Slender	S0	0L	SB-S0-0L	122.7	81.2	81.2	0.0	0.0	0.0	Shear
		0.5L	SB-S0-0.5L	154.7	102.4	81.2	0.0	21.2	26.1	Shear
		1L	SB-S0-1L	181.2	120.0	81.2	0.0	38.7	47.7	Shear
		2L	SB-S0-2L	183.8	121.7	81.2	0.0	40.4	49.8	Shear
	S1	0L	SB-S1-0L	397.0	262.8	81.2	181.6	0.0	0.0	Shear
		0.5L	SB-S1-0.5L	426.0	282.0	81.2	181.6	19.2	7.3	Shear
		1L	SB-S1-1L	385.2	255.0	81.2	181.6	—	0.0	Shear
		2L	SB-S1-2L	403.6	267.2	81.2	181.6	4.4	1.7	Shear
	S2	0L	SB-S2-0L	445.7	295.1	81.2	213.8	0.0	—	Flexure
		1L	SB-S2-1L	467.3	309.4	81.2	213.8	14.3	—	Flexure
		2L	SB-S2-2L	448.9	297.2	81.2	213.8	2.1	—	Flexure

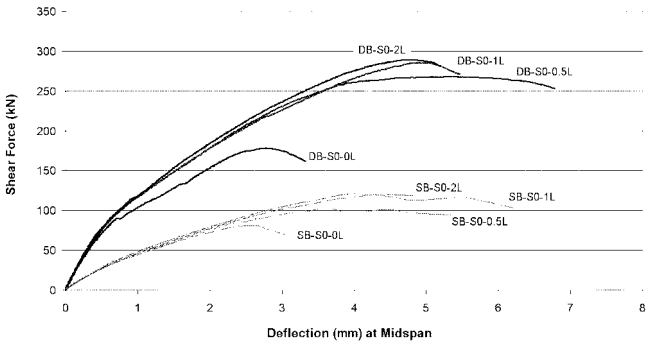

Fig. 4—Shear force versus midspan deflection—Series S0.

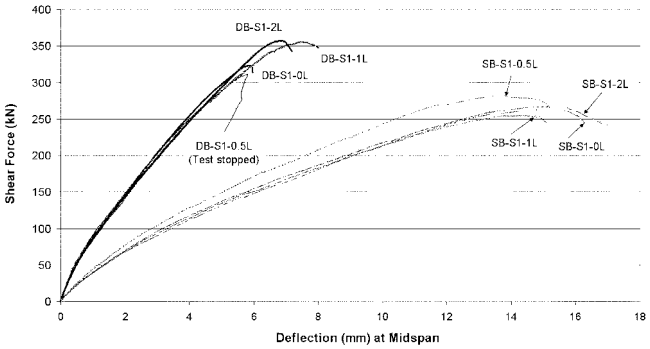

Fig. 5—Shear force versus midspan deflection—Series S1.

(Chaallal et al. 2002; Pellegrino and Modena 2002; Li et al. 2002) that the contribution of FRP to the shear resistance of a beam with transverse steel differs from that of the same beam but with no transverse steel. It is also observed that doubling the thickness (for example, from 0.5L to 1L or from 1L to 2L), does not lead to an additional shear capacity gain in proportion to the added CFRP as one would expect. For instance, for the specimens of Series SB-S0, the shear resistance gain, hereafter called the gain, increased from 26.1% for SB-S0-0.5L, to 47.7% for SB-S0-1L, and to 49.8% for SB-S0-2L. This result indicates that the gain due to the FRP is not in proportion to the FRP stiffness. However, the fact that the observed gain did not increase as the CFRP provided increased from one layer to two layers does not necessarily mean that the gain peaks as the FRP stiffness reaches a threshold. In this study, failure was due to crushing of concrete. Therefore, the gain peak due to FRP was dictated rather by the concrete compression strength than by the FRP stiffness. The shear capacity gain due to FRP, however, may also be limited by premature debonding due to high FRP stiffness, as observed by Triantafillou (1998).

It should be noted that the test on Specimen DB-S1-0.5L had to be interrupted due to a slight load imbalance observed at a fairly high applied load. Comparing the level of loading attained prior to interrupting the test with those of other specimens in the same series reveals that the load attained by the interrupted test specimen was near ultimate.

Deflection response

Figure 4 and 5 show the curves representing the shear force versus the midspan deflection for Series S0 and S1, respectively. The figures feature two distinct sets of curves corresponding to deep beams (upper curves) and slender beams (lower curves). The quasi-linear behavior of the curves is characteristic of a shear failure. Compared to slender specimens, the deep specimens featured a higher overall stiffness, but were more brittle (Fig. 5). Figure 5 reveals no overall gain in stiffness due to the CFRP on specimens with transverse steel. The specimens with no transverse steel showed a very minor change in overall stiffness due to the

CFRP (Fig. 4). Deep specimens with no transverse steel experienced slightly greater midspan deflections. The deflection ratio between the retrofitted specimens and those not retrofitted, however, is of the same order of magnitude, approximately 1.6, for both DB and SB categories. In contrast, with the presence of transverse steel, the deflection is substantially greater for slender beams, 14.6 mm on average, compared to deep specimens, which was only 6.5 mm on average.

Failure mode

All the tested specimens failed in shear, except those of Series SB-S2, which failed in flexure (refer to Table 5). No specimen failed by debonding, delamination, or fracture of the CFRP. The shear failure occurred by crushing of the concrete struts. In the retrofitted specimens, it was evident from the sudden appearance of a crack on the compression table (flange). This crack progressed rapidly and announced an imminent failure (Fig. 6). Note that in the specimens with transverse steel, crushing of concrete occurred after the transverse steel had yielded. Therefore, these specimens did not fail by premature crushing of concrete. Failure by flexure occurred by yielding of the longitudinal steel in the maximum moment zone, followed by crushing of the concrete in the compression zone at very large deformations (Fig. 6).

Cracking

In the deep specimens with no CFRP (DB-S0-0L, DB-S1-0L, and DB-S2-0L), cracking occurred at a shear force of approximately 80 kN. Specimen DB-S0-0L featured one principal crack propagating at an average angle of 36 degrees from the support to the load point, which is typical of deep beam behavior. In specimens with internal steel stirrups (DB-S1-0L and DB-S2-0L), in addition to the principal crack and parallel to it, other finer cracks developed (Fig. 7(a)). The ultimate load was attained as the principal crack extended deeper into the compression zone.

In the slender specimens with no CFRP (SB-S0-0L, SB-S1-0L, and SB-S2-0L), the cracking pattern depends on the transverse steel spacing. Specimen SB-S0-0L featured a principal crack that initiated at the support and progressed rapidly towards the compression zone at an angle of approximately 24 degrees (Fig. 7(d)). In Specimen SB-S1-0L (refer to Fig. 7(e)), cracking was rather widespread and propagated at a greater angle (with respect to longitudinal axis) compared to Specimen SB-S0-0L, because the crack angle increased from 24 to 38 degrees (Fig. 7(d)). In Specimen SB-S2-0L, which failed in flexure, the first flexural cracks appeared in the maximum moment zone at an applied shear force of 65 kN. The first diagonal cracks appeared in prolongation of flexural cracks at an applied shear force of approximately 100 kN, then stabilized at approximately 275 kN. The flexural cracks continued to progress within the maximum moment zone, until they reached the compression zone. This was then followed by crushing of the concrete at an applied shear force of approximately 295 kN.

In the retrofitted specimens with the U-shape continuous wrap adopted, the crack propagation could not be monitored during the course of the testing, except during the final phase of loading where cracks suddenly appeared on the compression table. At this stage, the applied load had already attained 95% of its ultimate value. Examination of the specimens after tests revealed an expansion of the concrete evidenced by a bulge within the cracking zone. To examine the concrete

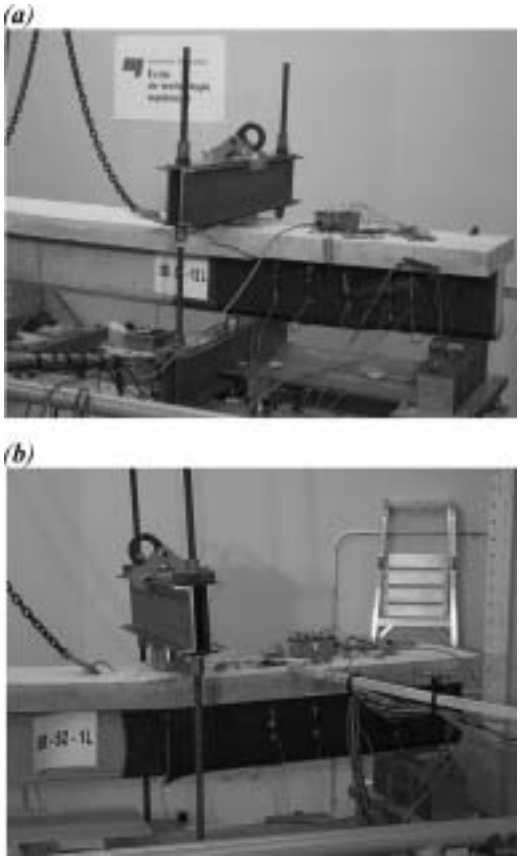

Fig. 6—Typical view of specimen at failure: (a) shear failure; and (b) flexural failure.

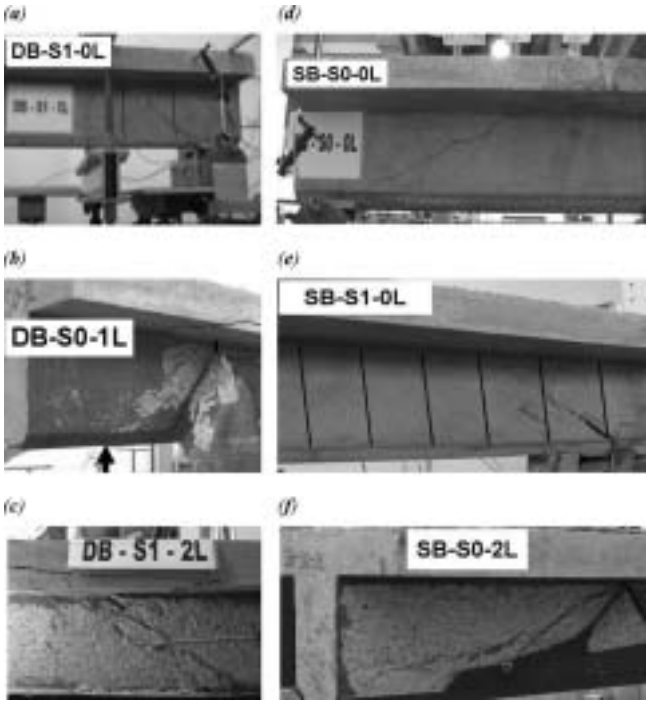

Fig. 7—Crack patterns at failure.

conditions, as well as the cracking pattern and extent, the CFRP wrap was carefully peeled off with some difficulty. The following observations were made: 1) The concrete was completely pulverized. Confined by the CFRP wrap, the concrete struts were subjected to stresses well beyond their

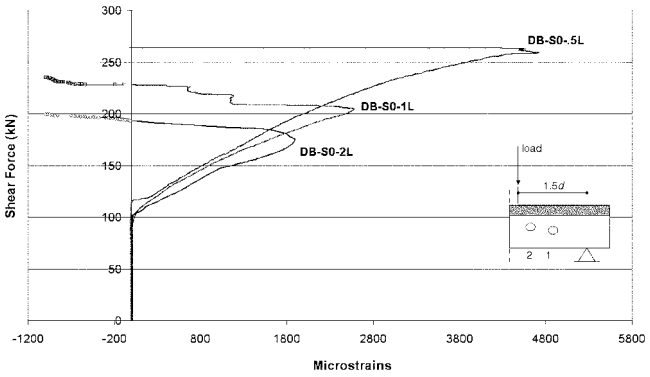

Fig. 8—Shear force versus vertical CFRP strains in terms of number of layers—deep beams, Series S0 (crack gauge 1).

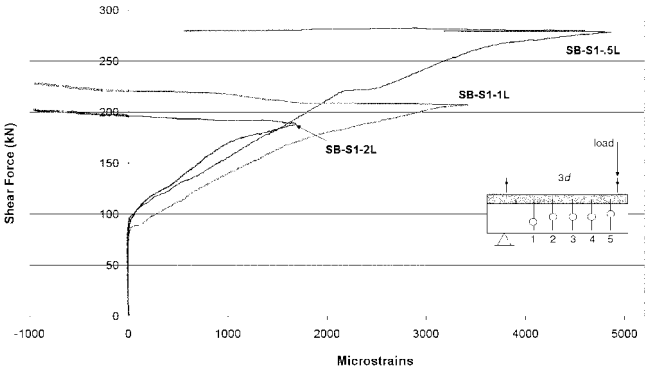

Fig. 9—Shear force versus vertical CFRP strains in terms of number of layers—slender beams, Series S1 (crack gauge 2).

compressive unconfined strength; 2) in deep specimens, one principal diagonal crack generally extended from the support zone to the point load zone (Fig. 7(b) and (c)). In some cases, however, in addition to this principal crack, a few fine diagonal cracks also developed. The crack angle was found to be approximately 36 degrees, that is, unchanged by the addition of the CFRP; and 3) in slender specimens pertaining to Series S0, only one principal crack was observed. As for Specimen SB-S0-0L, it was relatively less inclined, with a crack angle of approximately 22 degrees (Fig. 7(f)). In contrast, the specimens of Series S1, such as SB-S1-0L, showed rather widespread cracking, with an average crack angle of approximately 38 degrees. Again, it is seen that neither the cracking pattern nor the crack angle were modified by the CFRP retrofit.

The fact that in slender beams the cracking pattern is influenced by the presence of the transverse steel and not by that of the CFRP can be explained by the level of loading to failure attained in the case where transverse steel is present (refer to Table 5). A higher level of loading translates into more diagonal cracks prior to failure. In contrast, the specimens with no transverse steel experienced a lower level of loading to failure, which occurred well before diagonal cracks could proliferate within the test zone. In deep specimens, the presence of transverse steel and/or FRP did not alter the cracking pattern. This is attributed to the behavior of such deep specimens, where the transverse steel and/or the externally applied FRP contribute less to the shear resistance compared to slender specimens and may therefore affect the cracking pattern.

Finally, it may of interest to note that no crack was observed outside the tested zone of $a = 1.5d$ during the first test corresponding to a DB test (refer to Fig. 2(a)). Therefore, the segment of the beam specimen outside that zone was intact prior to the second test that is, SB test, refer to Fig. 2(b)).

Strains analysis

This part of the study investigates the behavior of the CFRP, the transverse steel, the longitudinal steel, and the concrete struts, as the thickness of the CFRP varies. As mentioned earlier, extensive instrumentation for strain monitoring was carefully engineered to provide the information and data much needed for the understanding of the shear resistance mechanisms involved in beams retrofitted with FRP. It must be realized that all the recorded data was subjected to careful examination, analysis, and comparisons. For obvious reasons, however, it is not possible to report all the findings in this paper. For more details, the reader is referred to Bousselham (2005).

CFRP strain—Figure 8 and 9 present the curves of the shear force versus the strains in the CFRP wrap for deep specimens with no transverse steel and for slender specimens with transverse steel spaced at $s = d/2$, respectively. For convenience, the locations of the strain gauges are provided along the curves in the figures. It is observed that the curves have the same tendency and feature three phases. In the initial stage of loading, the CFRP does not contribute to the load-carrying capacity. In the second stage, the CFRP begins to strain at an applied shear force of approximately 105 kN for deep specimens and 85 kN for slender specimens. The CFRP strain continued to increase under increasing applied shear force up to a certain threshold, the level of which differs from one specimen to another depending on the CFRP thickness (the thicker the CFRP, the lower this threshold level). In deep specimens for instance (Fig. 8), this level was 4720 microstrains in Specimen DB-S0-0.5L, 2580 microstrains in Specimen DB-S0-1L, and 1900 microstrains in Specimen DB-S0-2L. In the third stage, the CFRP strain started to decrease, drastically at times, as the shear force increased. This is shown by the reversing of the curves in Fig. 8 and 9 and can be explained as follows. Although no sign of debonding was observed during the course of the test, the few popping noises heard here and there lead to believe that local debonding could have occurred and may explain the CFRP strain decrease, which incidentally had no impact on the applied loading, which in fact continued to increase. It may be argued that the increase of the applied load is due to the so-called redistribution of loadings between the transverse steel and the concrete struts. This was not the case, however, because no related change has been observed in the behavior of these two components.

Transverse steel reinforcement strain—Figure 10 and 11 present for the deep and slender specimens, respectively, the curves for the applied shear force versus the strains in the transverse steel in terms of the CFRP thickness. These curves indicate that the behavior of the transverse steel went through three phases during loading. In the first initial phase, no noticeable contribution of the transverse steel to the resistance was observed. In the second phase, the first diagonal cracks initiated and the transverse steel started to strain. In the deep specimens, for instance, this phase started at an average applied shear force of approximately 75 kN for the control specimens, and 100 kN for the retrofitted specimens. The transverse steel strain continued to increase with increasing load until either the transverse steel yielded or rupture of the specimen occurred. In the third stage, the

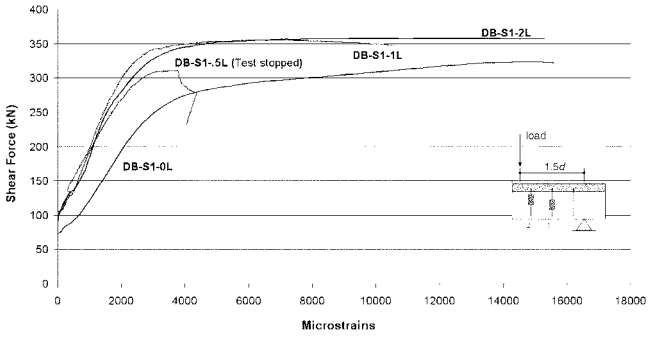

Fig. 10—Shear force versus transverse steel strain in terms of number of layers—deep beams (strain gauge 1).

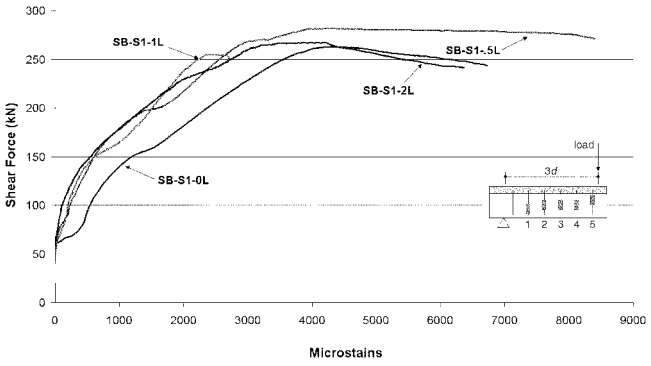

Fig. 11—Shear force versus transverse steel strain in terms of number of layers—slender beams (strain gauge 3).

transverse steel that yielded is easily identified by the large ductility plateau featured in the corresponding shear force-strain curves.

Given the applied load, the strain in the transverse steel was substantially greater in specimens with no CFRP. For slender specimens for instance, a difference of 1000 microstrains could be observed. Thus, it is seen that the presence of CFRP eased the strains in the transverse steel. Also, the yielding of the transverse steel occurred earlier in specimens with no CFRP in comparison to corresponding retrofitted specimens. It must be noted, however, that yielding of transverse steel was achieved in most cases, which is in agreement with the assumptions of the design guidelines (ACI Committee 440 2002; Canadian Standards Association 2002; *fib* TG 9.3 2001). This may provide an answer to the question raised on whether or not the assumption that steel stirrups attain yielding still hold true in the presence of FRP (Bousselham and Chaallal 2004).

Longitudinal steel reinforcement strain—The behavior of the longitudinal reinforcement at the location of the applied load point is illustrated in Fig. 12 and 13 for deep and slender specimens, respectively. It is observed that the longitudinal steel contributed very little to the resistance in the initial phase of the loading. As an example, this initial phase corresponds to 60 kN for deep specimens with no CFRP and extends to 70 kN when these specimens are retrofitted with two layers of CFRP. The slope change that characterizes the curves at the end of the initial phase announces the beginning of the second phase. The latter features a significant strain rate increase compared to the first phase. This transition phase gave rise to a rapid propagation of cracking of concrete in tension before the contribution to the resistance of the steel reinforcement effectively initiates. Then, the

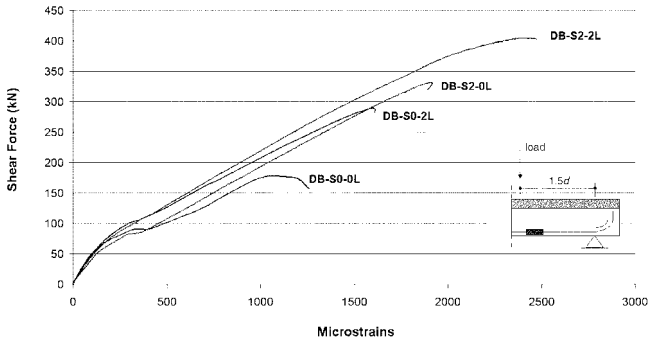

Fig. 12—Shear force versus longitudinal steel strain in terms of number of layers—deep beams (under load point).

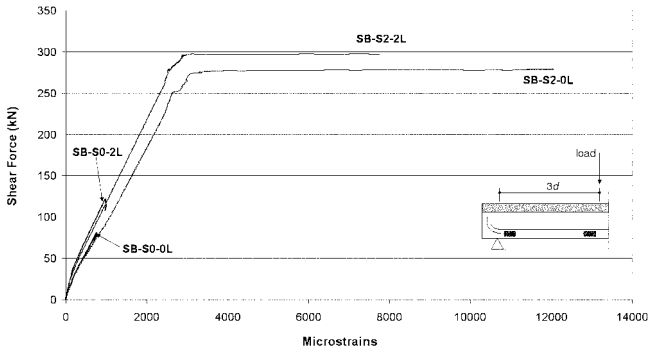

Fig. 13—Shear force versus longitudinal steel strain in terms of number of layers—slender beams (under load point).

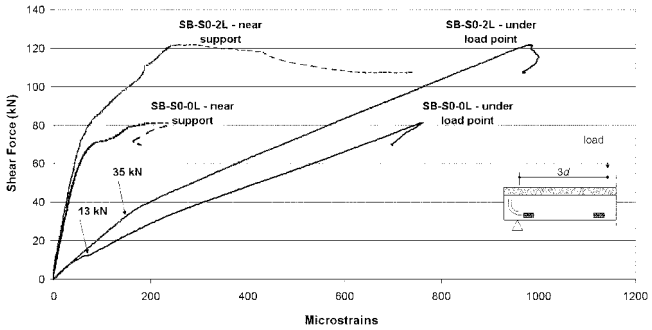

Fig. 14—Shear force versus longitudinal steel strain in slender beams—under load point versus near support.

applied load resumes its increase resulting in a linear response up to failure. Yielding of the longitudinal steel was never reached in any of the instrumented specimens, except for Series S2, where failure occurred by flexure. Therefore, specimens of Series S2 featured, as one would expect, a third phase governed by the plastic response of the longitudinal steel and characterized by a ductile plateau.

Figure 14 compares the response of the longitudinal steel located within the loaded zone with that located near the support zone for Specimens SB-S0-0L and SB-S0-2L. Note that only slender specimens had their longitudinal steel instrumented near the support zone. It is observed that for the longitudinal steel located within the loading zone, the contribution to the resistance initiated at an applied shear of approximately 13 kN for Specimen SB-S0-0L and 35 kN for Specimen SB-S0-2L. Physically, these loads caused the first cracks inside the loading zone. Thereafter, these cracks propagated towards the support where the longitudinal steel

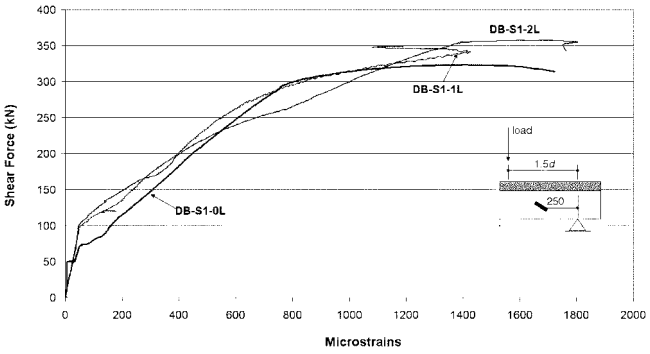

Fig. 15—Shear force versus concrete strain in terms of number of layers—deep beams.

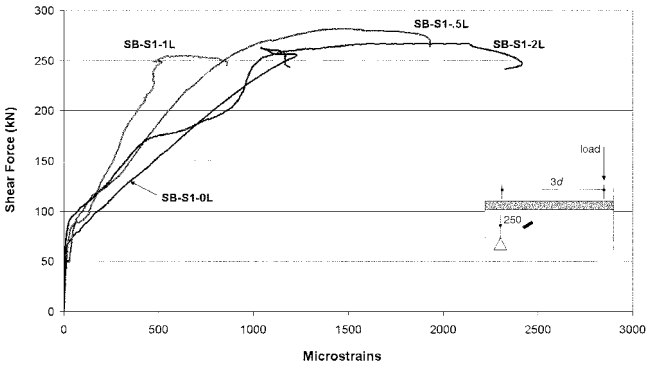

Fig. 16—Shear force versus concrete strain in terms of number of layers—slender beams.

started straining at applied shear forces of approximately 70 kN for Specimen SB-S0-0L, and 83 kN for Specimen SB-S0-2L. These forces are of the same order as those corresponding to the occurrence of diagonal cracks. This observation, which was also reported by Li et al. (2002), indicates the intimate relation that may exist between the cracking moment and the force corresponding to the first diagonal cracking, which incidentally is taken as the contribution of concrete to the shear capacity in some codes, such as ACI 318-02 (Joint ACI-ASCE Committee 426 1973).

As for the influence of the CFRP, given the applied load, the longitudinal steel seems somewhat less strained in retrofitted than in corresponding unretrofitted specimens (refer to Fig. 12 and 13). This is attributed to the CFRP on the tension face of the specimen, however, and not to that for the shear strengthening, at least for the U-wrap schemes used in this study.

Concrete strain—The curves representing the shear force versus the concrete strain measured on the concrete are presented in Fig. 15 and 16 in terms of the CFRP thickness, for deep and slender specimens, respectively. These curves, which feature similar forms, indicate that in the initial phase of loading, the compression concrete struts are practically not strained. This holds true up to an applied shear force of approximately 80 kN for specimens with no CFRP and 100 kN for specimens retrofitted with CFRP. These loads are of the same order as those corresponding to the initiation of strains in the transverse steel and/or in the CFRP. In other words, contributions of both the concrete struts and the transverse steel engage only after the diagonal cracks have developed. Consequently, and as noted by Park and Paulay (1975), the truss mechanism becomes effective only after the formation of the diagonal cracks. From then, it is observed that the strut strain increased almost linearly with increasing loads until it reached approximately 1000 microstrains, on average. Beyond that point, the curves featured a somewhat plastic response. Physically, this corresponds to the propagation of cracks towards the compression zone. The strut strain at failure attained 1200 to 1800 microstrains on average.

Table 6—Experimental versus predicted shear resistance due to CFRP

Beam type	Spacing	Specimen	Experimental, kN	CSA-S802, kN	ACI 440, kN	*fib* TG9.3, kN
Deep	S0	DB-S0-0.5L	90.1	24.7	24.7	39.3
		DB-S0-1L	107.4	44.1	40.8	50.5
		DB-S0-2L	110.9	88.2	62.4	68.5
	S1	DB-S1-0.5L	Stopped	24.7	24.7	39.3
		DB-S1-1L	32.0	44.1	40.8	50.5
		DB-S1-2L	34.2	88.2	62.4	68.5
	S2	DB-S2-1L	57.9	44.1	40.8	50.5
		DB-S2-2L	73.0	88.2	62.4	68.5
Slender	S0	SB-S0-0.5L	21.2	24.7	24.7	39.3
		SB-S0-1L	38.7	44.1	40.8	50.5
		SB-S0-2L	40.4	88.2	62.4	68.5
	S1	SB-S1-0.5L	19.2	24.7	24.7	39.3
		SB-S1-1L	0.0	44.1	40.8	50.5
		SB-S1-2L	4.4	88.2	62.4	68.5

Comparison of test results with shear design equations

The shear resistance due to the CFRP obtained by tests (refer to Table 5) is compared to the nominal shear resistance predicted by the guidelines in Table 6. Such a comparison is useful as it allows to verification of the reliability of the requirements contained in the codes and standards.

For slender specimens with no transverse steel (Series SB-S0), it is observed that the shear resistance obtained by tests is of the same order as the one predicted by both ACI 440.2R-02 and CSA-S806-02, for 0.5L and 1L. For these cases, the shear resistance predicted by *fib* TG9.3 is higher than the experimental value. In contrast, a significant deviation between experimental and guidelines values is observed for 2L schemes: while the gain obtained by test is negligible as the number of layers is increased from 1L to 2L, the guidelines overestimate the shear resistance. This is particularly true for the CSA-S806-02, where the prediction equations do not include the effect of the FRP stiffness. Generally, it can be concluded that the guidelines fail to adequately predict the shear resistance of strengthened beams when the thickness of FRP (and hence the stiffness) is high. In such cases, premature debonding can prevail, inhibiting thereby the gain due to FRP to reach its optimum value. Crushing of moderate strength concrete struts can also limit the gain due to FRP, as was the case for the specimens tested in this study. But this failure mode is not appropriately covered in the guidelines.

In contrast, for the slender specimens with transverse steel (SB-S1), the shear resistance due to FRP obtained by tests is negligible. This is not reflected in the guidelines because the shear resistance due to FRP is the same, regardless of the presence of transverse steel.

Likewise, the influence of the ratio a/d on the shear resistance due to FRP is clearly indicated by the test results but not included in the guidelines.

These observations are in agreement with the conclusions drawn by the authors (Bousselham at al. 2003), who compared, in an extensive state of the art review, more than a hundred test results reported in the literature with the values predicted by the guidelines. In these conclusions, it was noted that the research studies devoted to the shear strengthening yielded interesting results that were included in the guidelines. Nevertheless, it remains that comparison of the resistance predicted by the guidelines with test results clearly shows that major aspects, such as the transverse steel and the ratio a/d, are not captured by the guidelines.

CONCLUSIONS

This study presents results of an experimental investigation on the behavior of reinforced concrete T-beams retrofitted in shear with externally bonded CFRP composite. The influence of the following parameters was studied: 1) the CFRP ratio (that is, the number of CFRP layers); 2) the transverse steel ratio (that is, spacing); and 3) the shear length to the beam depth ratio, a/d (that is, deep beam effect). The following conclusions were reached:

1. The shear capacity gain due to the CFRP was greater for deep specimens than for slender specimens. This gain decreased with the addition of transverse steel. On the other hand, the shear capacity gain was not proportional to the CFRP thickness;

2. Neither the crack pattern, nor the crack angle was modified by the CFRP retrofit. For slender specimens, however, the presence of transverse steel affected both the crack pattern and angle;

3. Given the applied load, the strain in the transverse steel was substantially greater in specimens with no CFRP. However, the transverse steel yielded in most cases, as assumed by design codes and standards; and

4. Comparison of the resistance predicted by ACI 440.2R-02, CSA S806-02, and *fib*-TG9.3 with test results clearly shows that major aspects, such as the transverse steel, the FRP stiffness, and the ratio a/d, are not captured by the guidelines predictions.

It is hoped that the findings of this study contribute to the understanding of the shear resistance mechanisms involved in RC beams strengthened with externally bonded FRP. This understanding is of paramount importance, since it will ultimately lead to a more rigorous approach towards safer and rational design guidelines. It is recognized that this goal can only be achieved by including other equally important parameters that influence the shear resistance. The specimen scale factor is an example of one parameter that is currently being studied in the laboratory for Development and Research in Structures and Rehabilitation (DRSR) in Montreal.

ACKNOWLEDGMENTS

The financial support of the National Science and Engineering Research Council of Canada through an operating grant is gratefully acknowledged.

REFERENCES

ACI Committee 440, 2002, "Design and Construction of Externally Bonded FRP Systems for Strengthening Concrete Structures (440.2R-02)," American Concrete Institute, Farmington Hills, Mich., 45 pp.

Bakis, C. E.; Bank, L. C.; Brown, V. L.; Cosenza, E.; Davalos, J. F.; Lesko, J. J.; Machida, A.; Rizkalla, S. H.; and Triantafillou, T. C., 2002, "Fiber-Reinforced Polymer Composites for Construction—State-of-the-Art Review," *Journal of Composites for Construction*, V. 6, No. 2, pp. 73-187.

Bousselham, A., 2005, "Shear Strengthening Reinforced Concrete Beams with Fiber-Reinforced Polymer," PhD thesis, Department of Construction, École de technologie supérieure, Université du Québec, Montreal, Quebec, Canada, 420 pp. (in French)

Bousselham, A., and Chaallal, O., 2004, "Shear Strengthening Reinforced Concrete Beams with Fiber-Reinforced Polymer: Assessment of Influencing Parameters and Required Research, *ACI Structural Journal*, V. 101, No. 2, Mar.-Apr., pp. 219-227.

Bousselham, A.; Chaallal, O.; Hassan, M.; and Benmokrane, B., 2003, "Shear Strengthening of Concrete Structures with FRP: A Critical Review of Code Design Provisions," 31st Annual Conference, Canadian Society of Civil Engineers, Moncton, June 4-7. (CD-ROM)

Canadian Standards Association, 2002, "Design and Construction of Building Components with Fibre-Reinforced Polymer," CSA-S806-02, Rexdale, Ontario, Canada, 202 pp.

Chaallal, O.; Shahawy, M.; and Hassan, M., 2002, "Performance of Reinforced Concrete T-Girders Strengthened in Shear with Carbon Fiber-Reinforced Polymer Fabric," *ACI Structural Journal*, V. 99, No. 3, May-June, pp. 335-343.

Clarke, J. L., 2000, "The Use of Fibre Composites in Concrete Bridges: A State of the Art Review," *Technical Guide* No. 3, Concrete Bridge Development Group, 36 pp.

fib-TG9.3, 2001, "Design and Use of Externally Bonded Fiber Polymer Reinforcement (FRP EBR) for Reinforced Concrete Structures," *Bulletin* 14, 138 pp.

Joint ACI-ASCE Committee 426, 1973, "The Shear Strength of Reinforced Concrete Members," *Journal of the Structural Division*, V. 99, No. 6, pp. 1091-1187.

Khalifa, A., and Nanni, A., 2000, "Improving Shear Capacity of Existing RC T-Section Beams Using CFRP Composites," *Cement and Concrete Composites*, V. 22, pp. 165-174.

Li, A.; Diagana, C.; and Delmas, Y., 2002, "Shear Strengthening Effect by Bonded Composite Fabrics on RC Beams," *Composites Part B*, Elsevier, Chapter 33, pp. 225-239.

Matthys, S., and Triantafillou, T., 2001, "Shear and Torsion Strengthening with Externally Bonded FRP Reinforcement," *Proceedings of the International Workshop on Composites in Construction: A Reality*, E. Cosensa, G. Manfredi, and A. Nanni, eds., Capri, Italy, pp. 203-210.

Meier, U., 1995, "Strengthening of Structures Using Carbon Fibre/Epoxy Composites," *Construction and Building Materials*, V. 9, No. 6, pp. 341-351.

Neale, K. W., 2000, "FRPs for Structural Rehabilitation: A Survey of Recent Progress," *Progress in Structural Engineering and Materials*, V. 2, pp. 133-138.

Park, R., and Paulay, T., 1975, *Reinforced Concrete Structures*, Wiley, New York, 769 pp.

Pellegrino, C., and Modena, C., 2002, "Fiber Reinforced Polymer Shear Strengthening of RC Beams with Transverse Steel Reinforcement," *Journal of Composites for Construction*, V. 6, No. 2, pp. 104-111.

Triantafillou, T. C., 1998, "Shear Strengthening of Reinforced Concrete Beams Using Epoxy-Bonded FRP Composites," *ACI Structural Journal*, V. 95, No. 2, Mar.-Apr., pp. 107-115.

Triantafillou, T. C., and Antonopoulos, C. P., 2000, "Design of Concrete Flexural Members Strengthened in Shear With FRP," *Journal of Composites for Construction*, V. 4, No. 4, pp. 198-205.